Dielectric behavior induced by vitamin E and electron beam irradiation in ultra high molecular weight polyethylene

Journal:	*Journal of Applied Polymer Science*
Manuscript ID:	APP-2014-01-0137.R1
Wiley - Manuscript type:	Research Article
Keywords:	biomaterials, dielectric properties, crosslinking

Dielectric behavior induced by vitamin E and electron beam irradiation in ultra high molecular weight polyethylene

J.A. Puértolas[1], M.J. Martínez-Morlanes[1], R. Teruel[2], A. Martinez-Felipe[2], E. Oral[3], F.J. Pascual[1,4], A. Ribes[2]

[1]Department of Materials Science and Technology, I3A, Universidad de Zaragoza, Zaragoza, Spain
[2]Institute of Materials Technology, Universitat Politècnica de Valencia, Valencia, Spain
[3]Harris Orthopaedic Laboratory, Massachusetts General Hospital, Boston, MA, USA
[4]Centro Universitario de la Defensa de Zaragoza, Academia General Militar, Zaragoza, Spain.

*Correspondence to Prof. José A. Puértolas
Department of Materials Science and Technology,
Escuela de Ingeniería y Arquitectura-I3A, Universidad de Zaragoza,
E-50018, Zaragoza, Spain
Tel. : +34 976 762521
Fax. : +34 976 761957
e-mail: japr@unizar.es

ABSTRACT

Radiation cross-linked UHMWPEs have been successfully used as wear resistant bearing surfaces in total joint arthroplasty. A recent development in this field is the incorporation of the antioxidant vitamin E into radiation cross-linked UHMWPE. This study investigates the effects of radiation cross-linking and vitamin E incorporation on the dielectric behavior of UHMWPE. The dielectric relaxations of virgin and 0.1 wt% vitamin E blended UHMWPE and their irradiated counterparts (up to 300 kGy dose) were investigated. To determine the effect of vitamin E content alone, vitamin E loaded UHMWPEs were used. The results showed that radiation cross-linking and vitamin E content both increased dielectric polarization in UHMWPE and under some conditions induced electrical conductivity. This result is significant because it shows that the conductive response of UHMWPE bearing surfaces may depend on manufacturing processes and additives.

KEYWORDS: UHMWPE, polymer relaxations, dielectric behavior, vitamin E, α tocopherol, electron beam irradiation

INTRODUCTION

Dielectric relaxation spectroscopy (DRS) is a powerful tool to study the molecular dynamics in polymers.[1] This technique has also been applied to polyethylenes to understand the relaxation processes and to obtain the dielectric performance in applications where the dielectric insulation is a relevant parameter. In spite of the non polar character of this molecular structure, several complex relaxations named conventionally α, β and γ have been reported in the literature from higher to lower temperature due to the presence of other traces or polar groups in the polymer chain.[2-4] These units are introduced during the synthesis of the powder or during the consolidation process at high temperature and pressure. High density, low density or linear low density, HDPE, LDPE or LLDPE respectively, have been extensively studied in order to know the influence that different processes like crystallization, aging, irradiation, or the presence of antioxidants, blends, reinforcements or nano-reinfocements produce to the aforementioned relaxations.[5-8] In contrast to these studies related to polyethylenes, few works appeared in the literature concerning to the dielectric behavior of ultra high molecular weight polyethylene (UHMWPE), which presents a low dielectric constant and dielectric loss tangent.

Ultra high molecular weight polyethylene (UHMWPE) is a polymer that presents characteristics such as an excellent mechanical and tribological performance, high wear resistance, chemical inertness and biocompatibility, which have been exploited in different industrial areas and also as bearing parts in total joint replacements.[9] Besides, UHMWPE is a polyolefin with an effective behaviour in radiation shielding and therefore with potential application for spacecraft industry, or radiation–protective materials for personal and electronic equipments.[10]

Reinforced composite UHMWPE matrices have been developed for application in fields related to cosmic, proton, X-rays, electron or gamma irradiation devices.[11-13] On the other hand, electron beam irradiation process has been applied to UHMWPEs used as joint replacement parts to obtain a good sterilization method and to enhance the wear resistance behaviour by crosslinking the polymer chains.[14, 15] The introduction of antioxidants, like α-tocopherol (vitamin E), in UHMWPE by blending or diffusion, has been used as chemical stabilization since vitamin E exhibits a scavenger effect to the free radical induced by the irradiation. Electron beam irradiation and vitamin E incorporation, are being used to obtain first and second generation of commercially highly cross-linked polyethylenes.[16, 17]

This study analyses the changes in the dielectric properties and in the molecular dynamic of the UHMWPE with the incorporation of different vitamin E concentrations and under electron beam irradiation dose.

EXPERIMENTAL

The raw material used in this study was medical grade GUR1050 UHMWPE (Orthoplastics, UK). The vitamin E was incorporated in this polymer by blending and diffusion. The first method consisted of mixing UHMWPE powder with vitamin E at 0.1%wt. Prior to the mixture, vitamin E was dissolved in isopropyl alcohol (IPA) and the solution was mixed and stirred with the UHMWPE powder to make a homogeneous blend with a concentration of 2 wt% (weight percent). This blend was dried in a convection oven under vacuum at 60 ºC for 7 days and diluted with GUR1050 powders into 0.1 wt%. Finally, the last step consisted of consolidating the mixture into 9.5 mm-thick pucks under a specific program of temperature and pressure. To study the irradiation effects, these

molded blocks were subsequently irradiated by electron beam to 75, 150, 225 and 300 kGy (MT Cambridge, MA). After irradiation, all the specimens were maintained at -20 ºC in a subzero freezer until they were measured. Thus, hereafter, these materials will be referred to as GUR1050VE0.1-*X* kGy, where *X* is the former irradiation doses.

On the other hand, with the aim to study the effects of higher vitamin E concentrations, 0.2 mm sections were microtomed from the compression molded GUR1050 and soaked in a bath of vitamin E (α-tocopherol, Aldrich Chemicals) at 120 ºC in a nitrogen gas atmosphere for different times. At the end of the doping process, samples were taken out of the vitamin E bath, cleaned and subsequently homogenized at 120 ºC for 24 hours in nitrogen. In this case, the samples chosen for this study corresponding to concentrations of α-tocopherol of 1.4, 4.4 and 7.9 percent by weight. These materials will be designated as GUR1050-VE*Y*%, where *Y* is the former vitamin E concentrations.

Differential Scanning Calorimetry (DSC) was performed according to the ASTM F2625-10 standard[18] to assess thermal properties, namely crystallinity, melting and transition temperatures. Thus, three specimens (n=3) per material group were heated from 20 to 200 ºC at a rate of 10 ºC/min in a Differential Scanning Calorimeter (Perkin Elmer). Melting temperature, transition temperatures and crystallinity were obtained for each material.

Dielectric measurements were performed using a dielectric spectrometry setup (Novocontrol BDS4000), which includes a two-terminal dielectric cell, a frequency response analyser (Solartron 1250), and a high –impedance preamplifier of variable gain. The complex dielectric constant was obtained by sweeping the frequency range 0.01 Hz to 1MHz at different stabilized temperatures by heating from –70 ºC to 120 ºC in temperature

steps of 6 ºC. The samples were disks of a 0.2 mm thickness, which were held between the condenser plates (golden brass circular electrodes with a diameter of 11 mm).

The analysis was conducted through the complex dielectric permittivity $\varepsilon^* = \varepsilon' - i\varepsilon''$, taking into account the real, ε', and imaginary, ε'', parts, as well as tan $\delta = \varepsilon'' / \varepsilon'$. The results were expressed in the frequency, *f*, and the temperature, T, domains. The dielectric relaxations was analysed in the isotherms by fitting the response in the frequency domain to Havriliak-Negami (HN) curves (Eq. 1):[19-21]

$$\varepsilon^* - \varepsilon_\infty = \frac{\Delta\varepsilon}{\left\{1 + (iw\tau_{HN})^{\alpha}\right\}^{\beta}} \qquad (Eq1)$$

where *w* is the frequency in radians/second, α and β are parameters corresponding to the width and asymmetry of the relaxation time distributions, respectively; τ_{HN} is the Havriliak-Negami relaxation time and $\Delta\varepsilon = \varepsilon_S - \varepsilon_\infty$ the dielectric strength (with ε_S and ε_∞ are the real part of the permittivity when $w \rightarrow 0$ and $w \rightarrow \infty$, respectively). The relaxation time and frequency ($f_{max} = 1/\tau_{max}$) of the HN individual ε* curves were calculated according to Eq. 2:[19]

$$\tau_{\max} = \tau_{HN}\left[\frac{\sin\left(\frac{\pi(\alpha_{NH})\beta_{NH}}{2(\beta_{NH}+1)}\right)}{\sin\left(\frac{\pi(\alpha_{NH})}{2(\beta_{NH}+1)}\right)}\right]^{1/\alpha_{NH}} \qquad (Eq.2)$$

The ε'' curves were also fitted to Fouss-Kirkwood (Eq. 3) functions in the temperature domain:[22]

$$\varepsilon'' = \frac{\varepsilon''_{\max}}{\cosh\left\{bea\left(\frac{1}{T} - \frac{1}{T_{\max}}\right)\right\}} \qquad (Eq.3)$$

where bea = mE_a/R is a parameter dependent on the activation energy of the relaxation, E_a, ε''_{max} is the maximum in the ε″ curve and T_{max} the maximum relaxation temperature, at a given frequency (*f*).

At sufficiently high temperatures, ohmic conduction due to charge carriers, σ*, frequently dominates the loss contribution at low frequencies, potentially masking dielectric relaxations. In order to discriminate dielectric and conductivity effects, the conduction-free dielectric loss, ε''_{NC}, was also determined by Eq. 4:[23]

$$\varepsilon''_{NC} = \varepsilon'' - \frac{\sigma_0}{\varepsilon_0 2\pi f^S} \qquad (Eq.\ 4)$$

with f the frequency in Hertz, σ_0 a pre-exponential coefficient, and S an exponent normally close to 1.

The thermal activation of the dielectric phenomena was analysed in Arrhenius maps using the maxima temperature of the relaxations at each frequency or temperature, described by either linear (Eq. 5).

$$f_{max} = f_0 \exp\left(\frac{-Ea}{R \cdot T}\right) \qquad (Eq.\ 5)$$

where E_a is the apparent activation energy and f_0 is a pre-exponential term.

RESULTS AND DISCUSSION

Thermal results

The area below the thermograms from 50 to 160 ºC, normalized by 291 J/g as the enthalpy of melting of a 100 % crystalline UHMWPE, gave the crystallinity percentages for each material. Both the crystallinity and the peak melting point of 0.1 wt% vitamin E

blended polymer increased with radiation dose (**Table 1**). This trend was similar to previous reports for this resin without vitamin E.[24, 25]

On the other hand, the incorporation of vitamin E at high concentrations by diffusion (range 1.5-7.9 %wt) provoked a drop in the crystallinity content and lamellar thickness (**Table 1**). This last effect may be a consequence of the rise in transition temperature, T_m, which according to the Thomson-Gibbs equation involves in increasing in lamellar thickness, L_c:

$$T_m=T_{m0}\,(1-2\sigma/L_c\,\rho_c\,\Delta H_{m0})$$

where T_m is the melting point of the polymer; T_{m0} is the equilibrium melting point of a perfect crystalline polyethylene; σ, the specific surface energy; ρ_c, the crystallinity phase density and ΔH_{0m} the enthalpy of melting of a perfect crystalline polyethylene.

Finally, the reduction of crystallinity content due to the vitamin E has been also reported by Oral et al. 2007,[26] being this effect intensified when the temperature of the diffusion process approach to the melting temperature.

Dielectric results

The dielectric behaviour of resins without irradiation

Figure 1a shows the ε'' response corresponding to the GUR1050 sample, as a function of the temperature, and at different frequencies. At the lowest temperatures, the ε'' values are negligible and only at temperatures above 0 ºC and at frequencies lower than 10 Hz, some relaxations appeared. At the highest temperatures and lowest frequencies, the ε'' values rise, exceeding the range typical of dielectric relaxation and suggesting the existence of AC conductivity in that region. In case of GUR1050VE0.1 specimen, the

isochrone ε´´(T) curves show also (**Figure 1b**) several dielectric processes overlapped also with an AC conductivity term. The presence of this small vitamin E amount embossed the dielectric behaviour in ε´´ and additionally the appearance of a slight shift of the temperature of the ε´´ maximum to lower temperatures. The subtraction of conductivity term in both resins was performed by applying Eq. 4 in the frequency domain. The values of σ_0 and S at different temperatures are summarised in the first column of the **Tables 2a and 2b** for GUR1050VE0.1 and GUR1050, respectively. Although after the subtraction the values of ε´´(T, ω) cannon do not allow obtaining a reliable quantitative analysis of the relaxations present, dielectric measurements allow to detect some relaxations.

The γ relaxation is not observed in any of the materials, because it appears in the polyethylenes around -83 ºC, which is below of the lowermost temperature used during our experiment. The α and α´ relaxation, generally attributed to the relaxation mechanisms in the crystalline region, are observed in the unirradiated or uncross-linked resins, GUR1050 and GUR1050-VE0.1. The common β relaxation appears in some polyethylenes around -25 ºC is not detected in the neat GUR1050. This relaxation is widely accepted to be related to the relaxation of chain units in the interfacial zone between the lamella and its surrounding amorphous region.[27] Mechanisms associated to chain-end, fold-surface, branch-point molecular motions and chain rotation are involved in this relaxation.[5] Therefore, higher crystalline content, and the prevalent structural linearity of Nitta et al.[28] may result in the absence of this relaxation. However, in a recent work by Puértolas et al.[29] this β relaxation was weakly detected in GUR1050 by means of Dynamic Mechanical Thermal Analysis (DMTA).

Influence of the irradiation dose

The dielectric behaviour of the irradiated materials were similar that observed in the unirradiated material with respect to temperature and frequency. There were also two recognisable peaks at low frequencies, whose peaks do not follow a temperature/frequency dependence expected for relaxations. Additionally, a conductivity term is also present, which was also assessed by means of the same procedure described for the unirradiated material. The corresponding σ_0 and S values as a function of the temperature are included in **Table 2a**. The results indicated an increase in the conductivity values, σ_0, at the highest irradiation doses, reaching a value close to log σ_0 = -13 whereas all the values of the S parameter were close to 1. These AC conductivity outcomes showed higher radiation dose dependence than those found by Mathad et al.[30]

This conductivity could be associated with an increase of the carrier charge density as a result of an increase in free radicals, unsaturated bonds, defects, which may be generated by irradiation. However, the different mobility of the carrier in the amorphous and crystalline regions could be taken a synergetic effect on the different AC conductivity in the irradiated polyethylenes.

Influence of the Vitamin* E *concentration

Figure 2 is a 3D plot which illustrates the ε'' dependence of GUR1050-VE*Y*% series with Y = 1.3, 4.4 and 7.9 wt% of vitamin E content in the temperature and frequency range of interest. The plots show the presence of a relaxation at the lowest temperatures from -50 ºC to 20 ºC which is clearly visible for the specimens with Y = 4.4 and 7.9 wt%, but cannot be detected in the GUR1050-VE1.3 samples, suggesting that the relaxation must be related to the presence and amounts of Vitamin E. From the figures 2a, 2b, 2c can also be observed other process at higher temperatures and frequencies, which will be

denoted as α relaxation, rather a prominent conductivity is also present, especially above 20 ºC, which overlapped to the α relaxation.

The analysis of this process at the lowest frequencies applying the Eq. 4 allow us to determine the σ_0 and S parameter of the conductivity term, which are summarized in **Table 3**. At the same temperature, the conductivity is considerably higher in the sample with the highest Vitamin E contents, *Y*=7.9 w%, but the values are still lower those of the samples submitted to high dose irradiation.

In general, the AC conductivity presented a less significantly contribution when the vitamin E was incorporated into polyethylene by diffusion, than when the polyethylene resins underwent electron beam irradiation. In order to study the influence of the microstructure aspects on the AC conductivity, the first conclusion we deduce is that this AC conductivity is independent of the crystallinity, since the effects of electron beam irradiation and vitamin E content go in opposite trends respect the influence on crystallinity. In **Figure 3** we plot the log σ at different temperatures and corresponding to materials of both series (X and Y) versus their transition temperatures. According to this figure and take into account the relation of T_m and lamellar thickness (see Thomson-Gibbs equation), it seem that the lamellar thickness is a relevant microstructural factor for the AC conductivity, in the same line that the conclusion given by Mandelkern et al.[27]

The subtraction of the conductivity term from the isothermal curves, ε´´(f) above 51 ºC, revealed the presence of the α process, which is especially visible in the case of GUR1050-VE7.9, and whose intensity increases with increasing temperature. The results also point out that the isothermal curves undergoes changes in the peak shape in a more significant way than the peak position, with an additional growing component at around *f*

= 3 Hz. However, the uncertainty of the experimental values of ε´´ does not allow a reliable information of this complex process.

Dielectric response at lower temperatures was not affected by conductivity, therefore the analysis of this relaxation was less complicated. Henceforth this relaxation will be denoted as β relaxation. **Figure 4** shows the isochronal curves. Isothermal curves values were fitted to Havriliak-Negami (*Eq.1* and *2*) and isochronal ones by Fouss-Kirkwood (*Eq. 3*) equations, respectively and the parameters obtained are indicated in **Tables 4 and 5**. The relaxation times (τ_{max}) and temperatures (T_{max}) determined with Eq. 1, 2 and 3, respectively, were used to plot the corresponding Arrhenius maps in **Figure 5**. The β relaxations show linear dependence with the temperature, indicating low influence of cooperative motions in the dielectric response, being in good coherence with the results obtained by NH and FK because the error band was lower than 10%. Activation energies calculated following *Eq. 6*, are summarised in **Table 4**.

Few works have focused on the dielectric contribution of α-tocopherol, which is the compound incorporated into UHMWPE by blending into resin powder before consolidation or diffusion into consolidated solid forms. This tocopherol is a glass-forming material with a glass transition close to -33 ºC. The introduction of 0.1 wt% vitamin E by blending in the polyethylene does not modify the previous behavior regarding the absence of the β relaxations. However, in the non irradiated vitamin E diffused polyethylene, above 1.5 wt% of vitamin E these materials exhibit the β relaxation, which was strengthened by increasing the amount of vitamin E doping and was shifted toward low temperatures. These results corroborate earlier results on the effect of diffused vitamin E on the relaxation behavior of UHMWPE obtained by DTMA.[22] Besides, the activation energy, which is around 184 $kJmol^{-1}$ by means of the Fouss-

Kirkwood approach, is close to the previously determined from T_{max} of the isochrone curves, 188 $kJmol^{-1}$ at 9 wt% in that work. Regardless of the used technique, DRS or DMTA, the rising activation energy registered for increasingly higher antioxidant concentrations seem to discard any plasticization effect of vitamin E in spite of the temperature shift of the β relaxation.

It is difficult to associate the origin of this β relaxation with the presence of the vitamin E. A possible mechanism could be related to the microstructural changes induced by the annealing at 120°C, which is used during the incorporation of vitamin E into polyethylene.[31, 32] Although chain scissions take place initially in the amorphous zone, the morphological changes are mainly produced in the crystalline- amorphous interface. Thus, these changes together with possible recrystallization of newly formed chains may modify crystalline-amorphous interface in the presence of high concentration of vitamin E and contribute to the induction of a β relaxation.

CONCLUSIONS

The α and α´ relaxation are overlapped by AC conductivity that is present about 60 ºC for all the studied materials. This AC conductivity increased clearly when the polyethylene resins underwent electron beam irradiation and less significantly when the vitamin E was incorporated into polyethylene by diffusion from its respective basic resins.

The effects of electron beam irradiation and vitamin E content go in opposite trends. The lamellar thickness is a relevant microstructural factor of α and α´ relaxation

The β relaxation is not detected in the neat GUR1050 and 0.1 wt% vitamin E by blending in the polyethylene. However, in the non-irradiated vitamin E diffused polyethylene, above 1.5 wt% of vitamin E these materials exhibit the β relaxation, which

was strengthened by increasing the amount of vitamin E doping and was shifted toward low temperatures. A possible mechanism could be related via the microstructural changes induced by the incorporation of the vitamin E infused polyethylene, simultaneously to the annealing process at 120 ºC.

REFERENCES

1. Boyd, R.H.; Smith, G.D. Polymer Dynamics and Relaxation; Cambridge University Press: Cambridge, **2007**.
2. Schmieder, K.; Wolf, K. Kolloid Z. **1953**, 134, 149.
3. Oakes, W.G.; Robinson, D.W.; J. Polymer. Sci. **1954**, 14, 505.
4. Flocke, H.A. Kolloid Z. **1962**, 180, 118.
5. Suljovrujic. E. Radiat. Phys. Chem. **2010**, 79, 751.
6. Gilchrist. J. le G. Cryogenics **1979**, 19, 281.
7. Yang, S.; Benitez, R.; Fuentes, A.; Lozano. K. Compos. Sci. Technol. **2007**, 67, 1159.
8. Suljovrujic, E.; Kacœarevic-Popovic, Z.; Kostoskia, D.; Dojcœilovic. J. Polym. Degrad. Stabil. **2001**, 71, 367.
9. Kurtz, S. M. The UHMWPE Biomaterials Handbook: Ultra- High Molecular Weight Polyethylene in Total Joint Replacement and Medical Devices, 2nd ed.; Academic Press: Burlington, MA, **2009**.
10. Cumming, C.S.; Lucas, E.M,; Marro, J.A.; Kieu, T.M.; DesJardins, J.D. Adv. Space Res. **2011**, 48, 1572.
11. Zhong, W.H.; Millert, J. International Conference on Smart Materials and Nanotechnology in Enginnering V6423:Z4231, **2011**.
12. Cao, X.Z.; Xue, X.X.; Jiang, T.; Li, Z.F.; Ding, Y.F.; Li, Y.; Yang, H. J. Rare Earths **2010**, 28S1:482.
13. Kaloshkin, S.D.; Tcheerdyntsev, V.V.; Gorshenkov, M.V.; Gulbin, V.N.; Kuznetsov, S.A. J. Alloy. Compd. **2012,** 536S:522-S526.
14. Muratoglu, O.K.; Bragdon, C.R.; O´Connor, D.; Perinchief, R.S.; Estok, D.M.; Jasty, M.; Harris, W.H. J. Arthroplast. **2001**, 16, 24-30.
15. Goldman, M.; Gronsky, R.; Pruitt, L. J. Mat. Sci-Mat Med **1998**, 98, 207-212.

16. Gómez-Barrena, E.; Puértolas, J.A.; Munuera, L.; Konttinen, Y. Acta Orthop. **200**8, 79:832.
17. Bracco, P.; Oral, E. Clin. Orthop. Rel. Res. **2011**, 469, 2286-2293.
18. ASTM F2625. Standard test method for measurement of enthalpy of fusion, percent crystallinity, and melting point of ultra-high-molecular weight polyethylene by means of differential scanning calorimetry.
19. Havriliak, S.; Negami, S. A. Polymer **1967**, 8, 161.
20. Havriliak, S.; Negami, S. In Dielectric and Mechanical Relaxation in Materials; Hanser: Munich, **1997**.
21. Ngai, K.L.; Schonhals, A.; Schlosser, E. Macromolecules **1992**, 25, 4915.
22. Fuoss, R.M.; Kirkwood, J.G. J. Am. Chem. Soc. **1941,** 2, 385.
23. Brottcher, C.J.F.; Borderwijk, P. In Theory of Electric Polarization, 2nd ed.; Elsevier: Amsterdam, **1978**.
24. Premnath, V.; Harris, W.H.; Jasty, M.; Merrill, E.W. Biomaterials **1996**, 17, 1741.
25. Medel, F.J.; García-Álvarez, F.; Gómez-Barrena, E.; Puértolas, J.A. Polym. Degrad. Stabil. **2005**, 88, 435.
26. Oral, E.; Wannomae, K.K.; Rowell, S.L.; Muratoglu, O.K. Biomaterials **2007**, 28, 5225.
27. Mandelkern, L.; Glotin, M.; Popli, R. J. Polym. Sci. Polym. Phys. **1981**, 19, 435.
28. Nitta, K.H., Tanaka, A. Polymer **2001**, 42, 1219.
29. Puértolas, J.A.; Martínez-Morlanes, M.J.; Mariscal, M.D.; Medel, F.J. J. Appl. Polym. Sci. **2011**, 120, 2282.
30. Mathad, R.D.; Kumar, H.G.H.; Sannakki, B.; Sanjeev, G.; Sarma, K.S.S.; Francis, S. Radiat. Eff. Defect. S. 2010, 165, 277.
31. Ribes-Greus, A.; Díaz-Calleja, R. J. Appl. Polym. Sci. **1989**, 38, 1127.
32. Ribes-Greus, A.; Díaz-Calleja, R. J. Appl. Polym. Sci. **1989**, 37, 2549.

ACKNOWLEDGEMENTS

Research funded by the Comisión Interministerial de Ciencia y Tecnología (CICYT), Spain. Project: MAT 2010-16175 from the Ministerio de Ciencia e Innovación.

FIGURE CAPTIONS

Figures 1a and 1b. Temperature dependence of the imaginary part of ε´´(T) in a) GUR1050, b) GUR1050VE0.1, at different frequencies: (□) $3x10^4$, (○) $3x10^3$, (▲) 30, (x) 10, (+) 3, (♦) 0.3, (▼) 0.1, and (●) 0.03Hz.

Figure 2. 3D plots showing the frequency/temperature dependence of the ε″ response of (a) GUR1050-VE1.3 (b) GUR 1050-VE4.4 and (c) GUR 1050-VE7.9.

Figure 3. AC conductivity at different temperatures in function of the temperature transition in all the studied materials.

Figure 4. Temperature dependence of the ε″ response of GUR1050-VE4.4 (left) and GUR 1050-VE7.9 (right) in the low temperatures range, at different frequencies (in Hz): ■ $1x10^4$, ◆ $3x10^3$, ▲ $1x10^3$, ● $3x10^2$, ■ $1x10^2$, ◆ $3x10^1$, ▲ $1x10^1$, ● $3x10^0$, □ $3x10^{-1}$, and ◇ $1x10^{-1}$.

Figure 5. Arrhenius maps corresponding to the, GUR1050-VE4.4 (left) and GUR1050-VE7.9 (right) samples, obtained from the application of the Fouss-Kirwood (■) and Havriliak-Negami (♦) equations.

TABLE CAPTIONS

Table 1. Influence of gamma irradiation doses and vitamin E content on thermal parameters of electron beam irradiated GUR1050VE0.1 and vitamin E diffused GUR1050.

Table 2. Influence of electron beam irradiation on AC conductivity parameters obtained by Eq.4 in GUR1050VE0.1-*X* kGy.

Table 3. Influence of vitamin E content on AC conductivity parameters obtained by Eq. 4 in GUR1050-*Y* wt%.

Table 4. Parameters obtained after fitting the ε″ curves to Havriliak-Negami expressions.

Table 5. Parameters obtained after fitting the ε″ curves to Fouss-Kirkwood expressions.

Table 6. Activation energies, Ea, calculated for the low temperature relaxation in GUR1050.

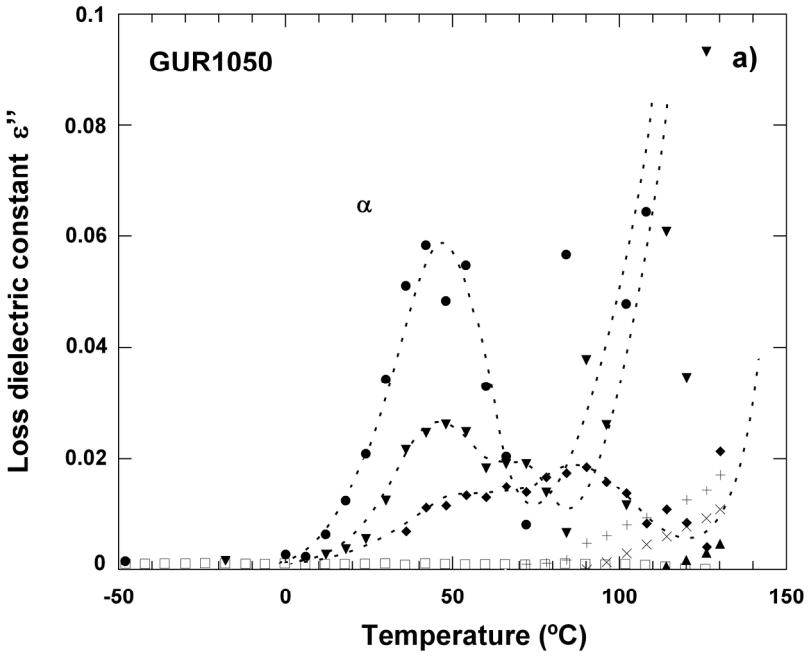

Figure 1a
189x157mm (300 x 300 DPI)

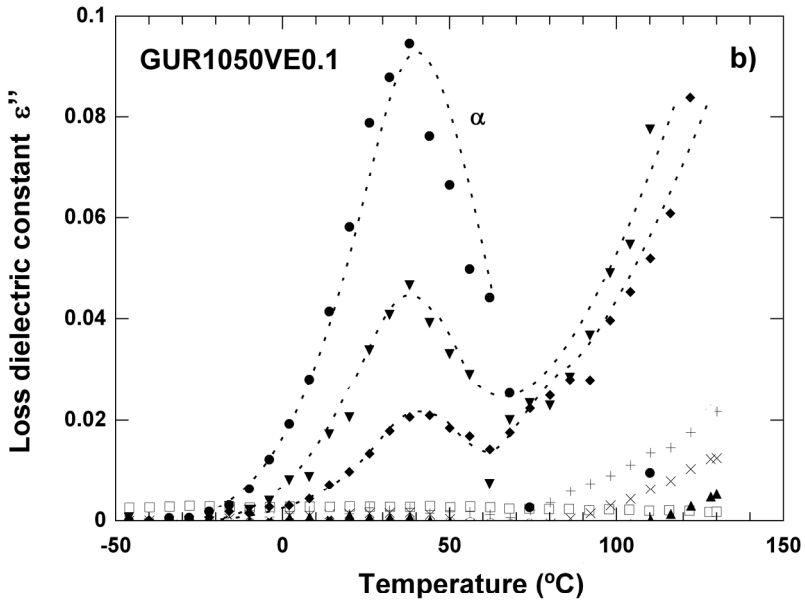

Figure 1b
189x157mm (300 x 300 DPI)

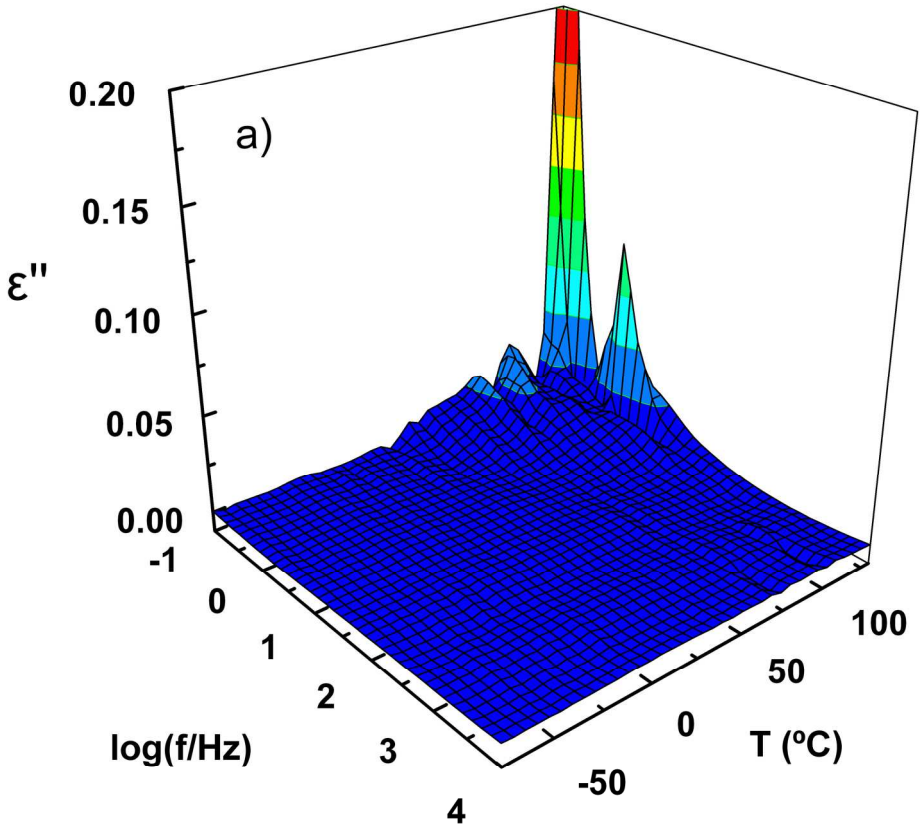

Figure 2a
177x155mm (300 x 300 DPI)

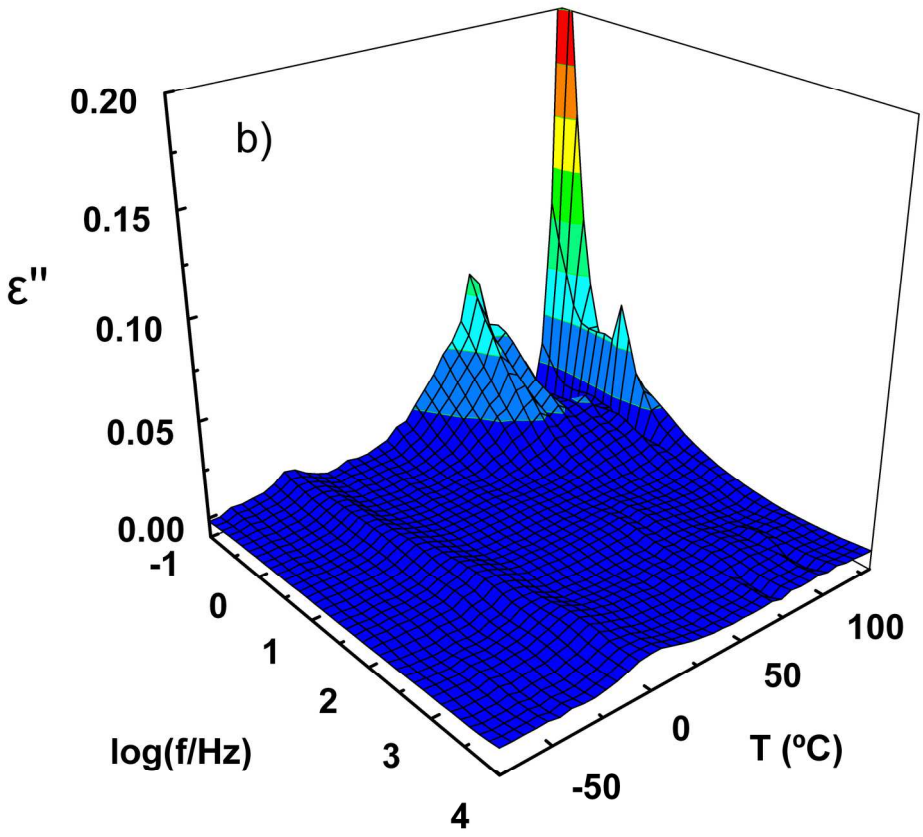

Figure 2b
177x155mm (300 x 300 DPI)

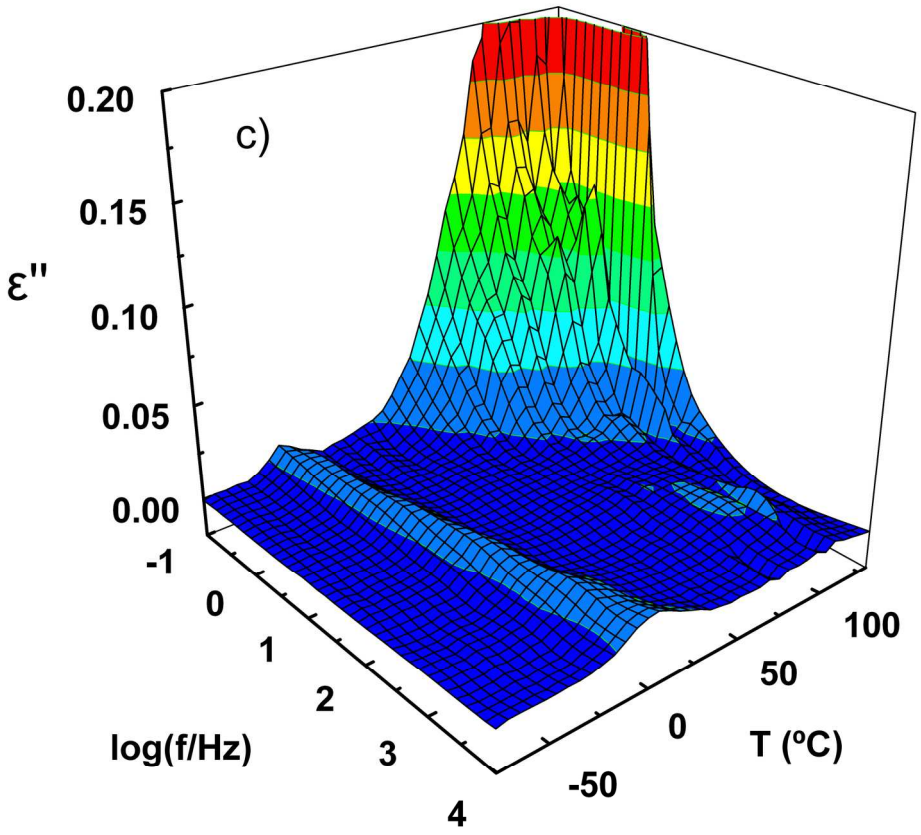

Figure 2c
177x155mm (300 x 300 DPI)

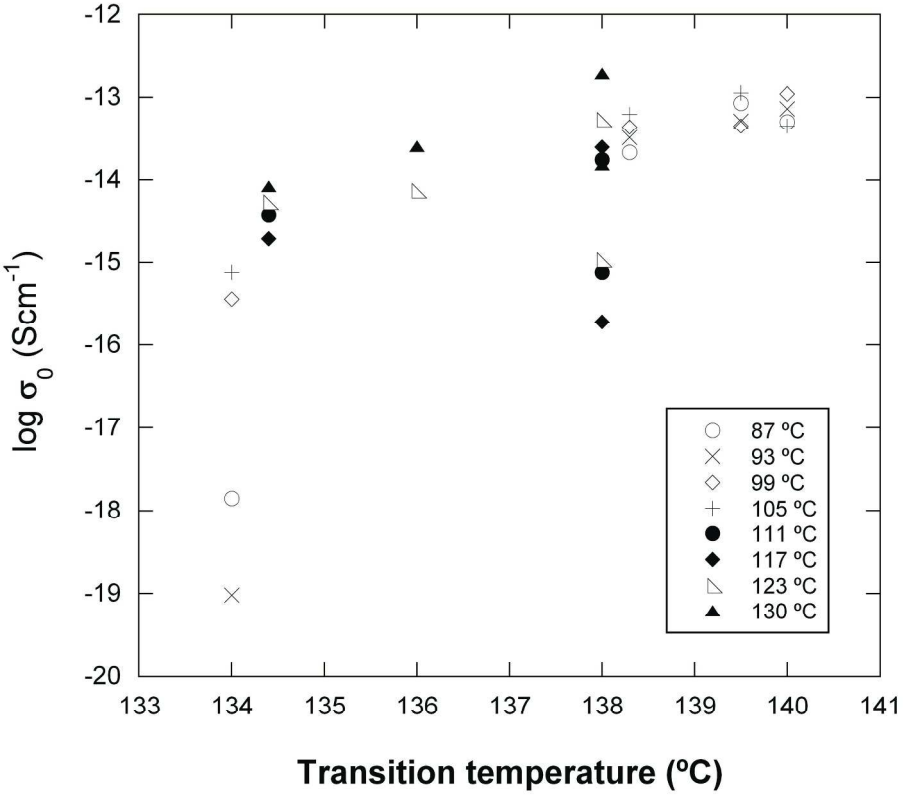

Figure 3
122x106mm (600 x 600 DPI)

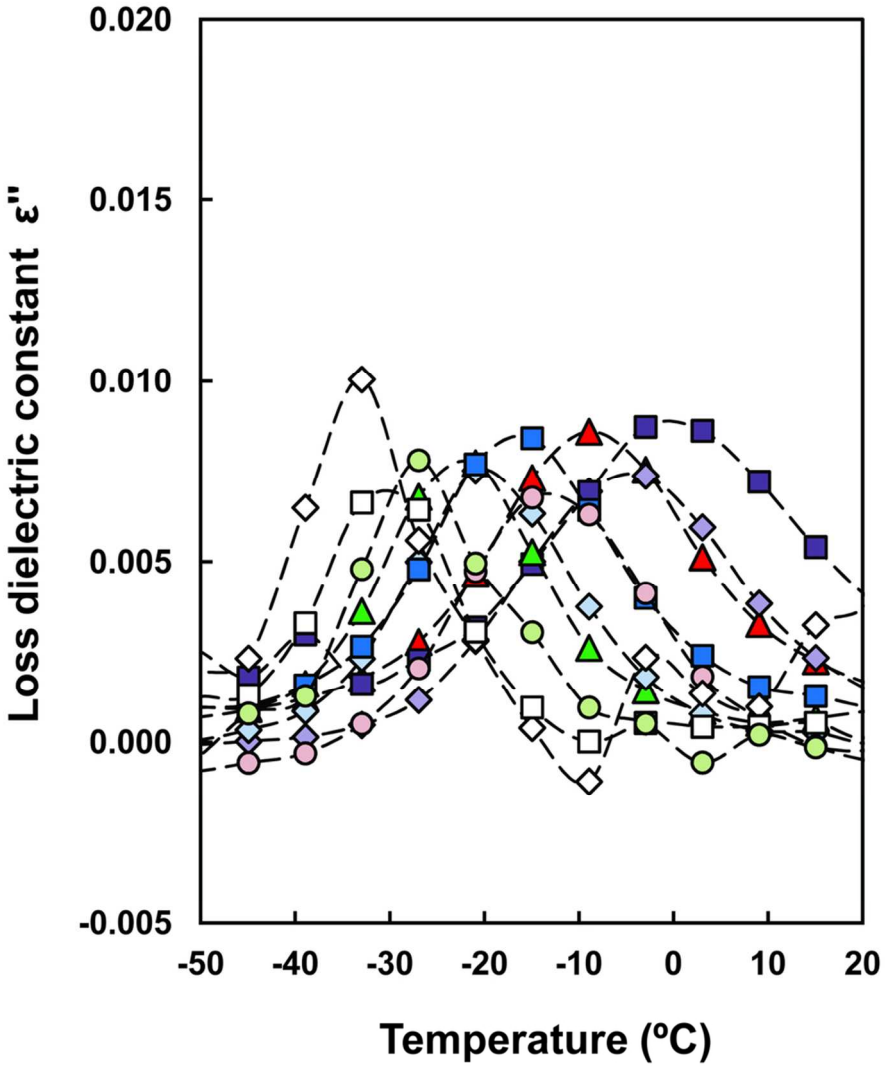

Figure 4a
92x107mm (300 x 300 DPI)

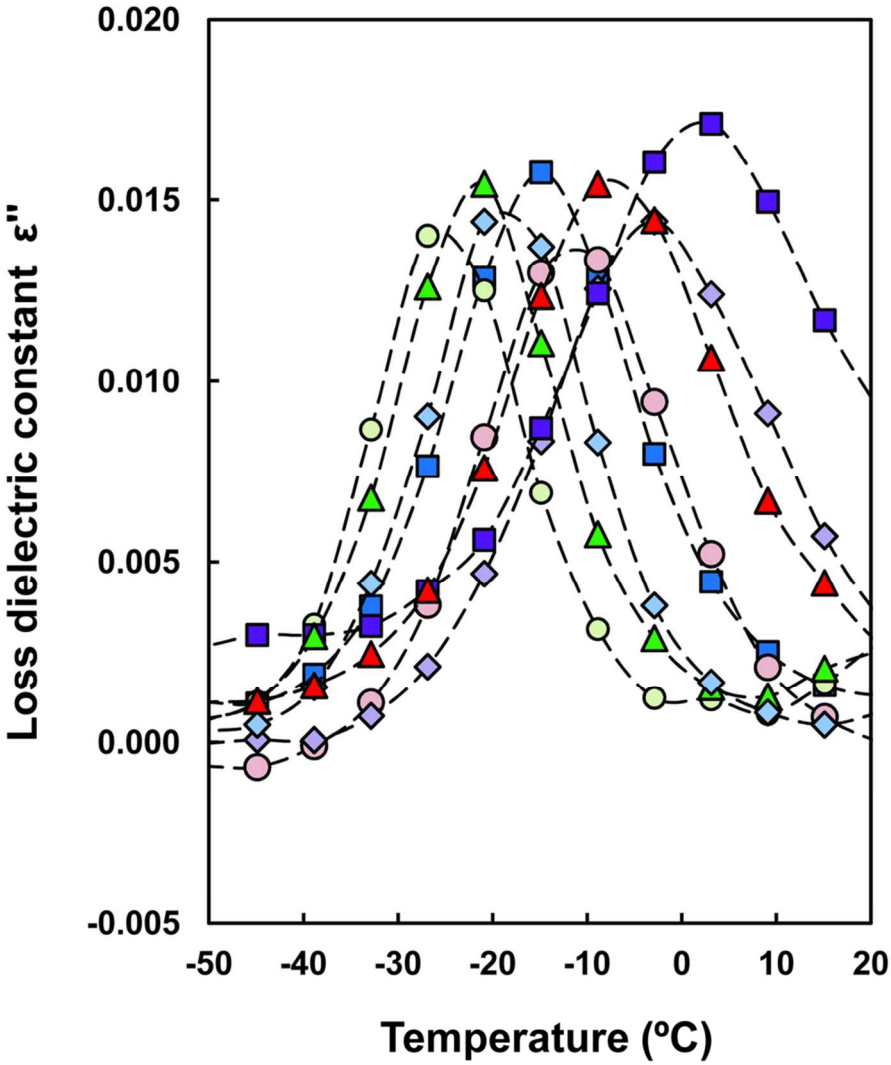

Figure 4b
92x107mm (300 x 300 DPI)

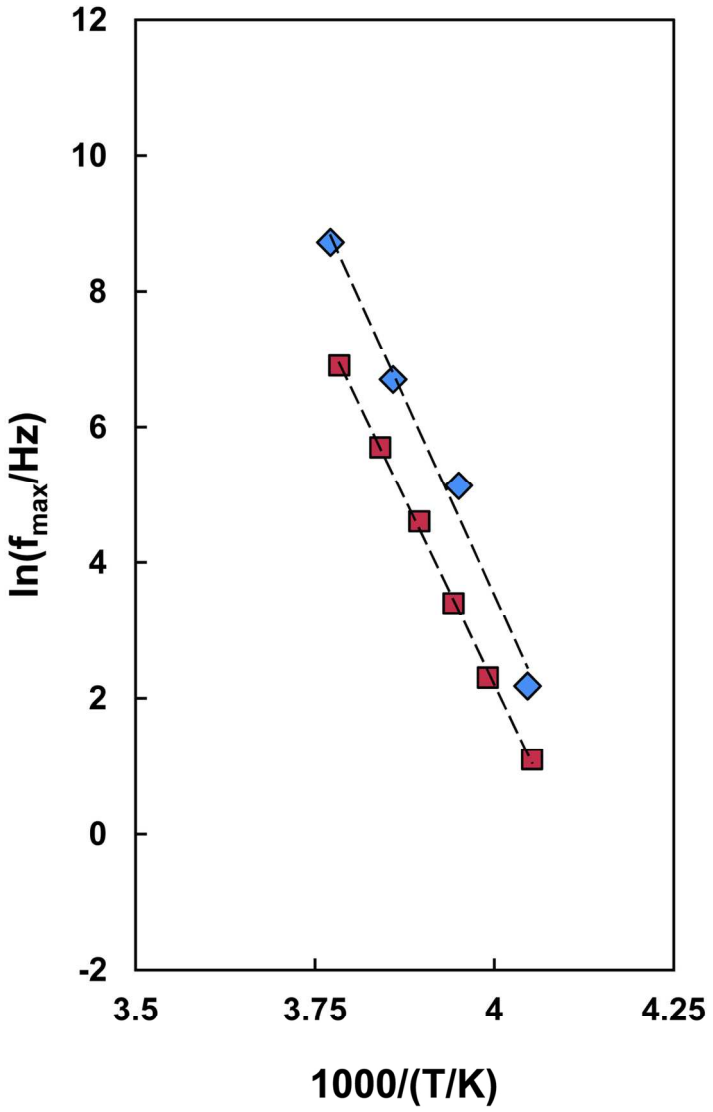

Figure 5a
120x182mm (300 x 300 DPI)

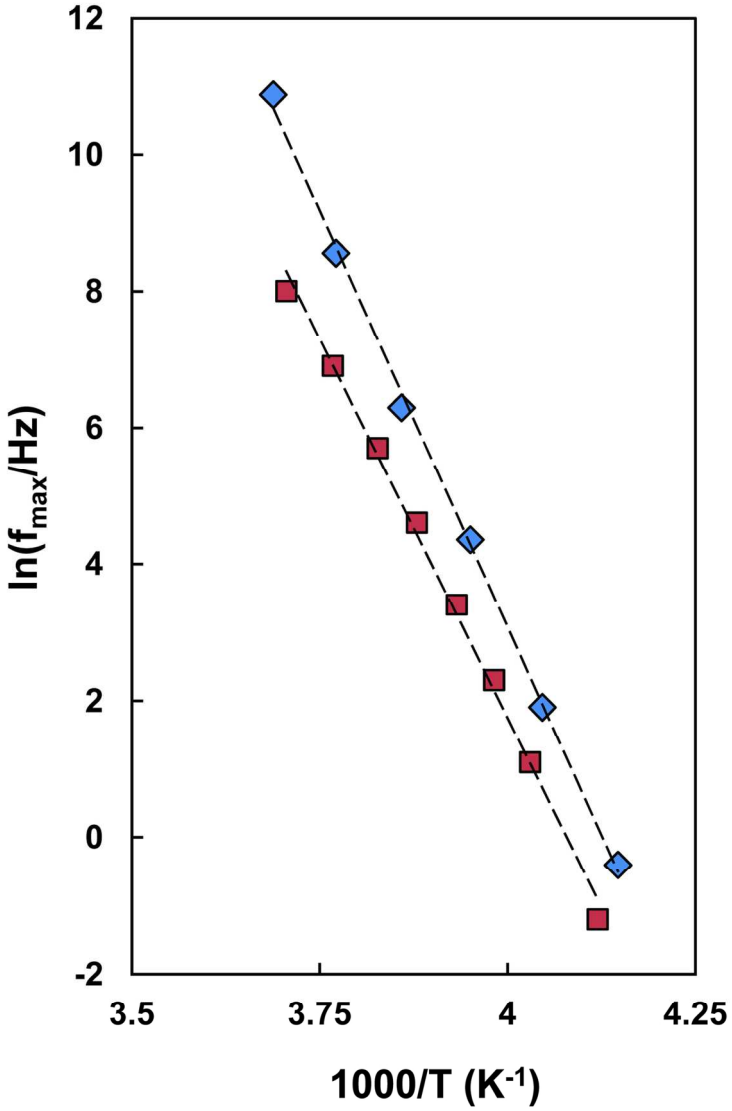

Figure 5b
120x182mm (300 x 300 DPI)

Table 1. Influence of gamma irradiation doses and vitamin E content on thermal parameters of electron beam irradiated GUR1050VE0.1 and vitamin E diffused GUR1050.

Doses (kGy)					
	0	75	150	225	300
Crystallinity (%)	52.5±1.0	56.5±0.5	56.8±1.8	57.7±0.9	56.2±3.1
Transition temperature (ºC)	134.3±0.2	137.0±0.1	138.3±0.1	139.5±0.1	140.0±0.5
Vitamin E (wt %)					
	0	1.5	4.4	7.9	
Crystallinity (%)	50.3±0.9	49.8±1.0	46.8±0.7	45.3±0.7	
Transition temperature (ºC)	134.3±0.2	134.2±0.5	138.3±0.3	137.9±0.1	

Table 2. Influence of electron beam irradiation on AC conductivity parameters obtained by Eq.4 in GUR1050VE0.1-*X* kGy.

T (ºC)	$\log(\sigma_0/(S\cdot cm^{-1}))$				S			
	0 kGy	**150 kGy**	**225 kGy**	**300 kGy**	**0kGy**	**150kGy**	**225kGy**	**300 kGy**
130	-13.72		-12.09	-11.80	1.00		0.75	0.85
123	-13.95		-12.11	-12.10	0.93		0.74	0.87
117	-14.05		-12.49	-12.34	0.97		0.86	0.86
111	-14.07		-12.88	-12.56	1.00		0.89	0.86
105	-15.12	-13.21	-12.95	-13.35	1.00	0.91	0.86	0.76
99		-13.36	-13.35	-12.96		1.00	0.76	0.89
93		-13.49	-13.29	-13.14		1.00	0.84	0.85
87		-13.67	-13.07	-13.30		0.90	0.89	0.84
81		-13.78	-13.32	-13.50		1.00	0.91	0.78
75		-14.02	-13.61	-13.67		1.00	0.87	1.00
69		-14.40	-13.95	-14.07		0.93	0.85	0.68
63		-14.66	-14.18	-14.27		1.00	1.00	0.76
57		-14.96	-14.55	-14.46		1.00	0.97	0.78
51		-14.97	-15.76	-14.55		1.00	1.00	0.87

Table 3. Influence of vitamin E content on AC conductivity parameters obtained by Eq. 4 in GUR1050-*Y* wt%.

T (ºC)	$\log(\sigma_0 /(S \cdot cm^{-1}))$				S			
	0 wt%	**1.5 wt%**	**4.4 wt%**	**7.9 wt%**	**0 wt%**	**1.5 wt%**	**4.4 wt%**	**7.9 wt%**
130	-14.08	-13.60	-13.82	-12.72	1.0	1.00	0.96	0.90
123	-14.27	-14.13	-14.97	-13.27	1.0	1.00	0.69	0.84
117	-14.72		-15.72	-13.61	1.0		0.76	0.81
111	-14.42		-15.12	-13.76	1.0		1.00	0.81
105			-15.05	-14.06			1.00	0.70
99				-14.03			1.00	0.79
93				-13.93				0.98
87				-14.02				0.94
81				-14.16				0.84
75				-14.09				1.00
69				-14.25				0.93
63				-14.19				1.00
57				-14.52				0.87
51				-14.57				1.00

Table 4. Parameters obtained after fitting the ε″ curves to Havriliak-Negami expressions.

	GUR1050-VE4.4				GUR1050-VE7.9			
T (°C)	**τ_{max} (sec·10^2)**	**$\Delta\varepsilon''$ (·10^2)**	**α**	**β**	**τ_{max} (sec·10^2)**	**$\Delta\varepsilon''$ (·10^2)**	**α**	**β**
-32	314000	7.27	0.76	0.34				
-26	11300	54.9	0.82	0.29	14900	0.360	0.51	0.54
-20	591	2.81	0.45	0.69	1280	1.02	0.44	0.78
-14	123	0.903	0.59	0.37	185	0.765	0.62	0.30
-8	16.4	0.0897	0.49	0.46	19.3	0.306	0.71	0.11
-2	1.06	0.00579	0.44	0.60				

Table 5. Parameters obtained after fitting the ε″ curves to Fouss-Kirkwood expressions.

	GUR1050-VE4.4			GUR1050-VE7.9		
f **(Hz)**	$\varepsilon_{max} \cdot 10^3$	**bea**	T_{max} (ºC)	ε_{max}	**bea**	T_{max} (ºC)
3	7.77	10260.14	-26.4	14.53	8607.12	-30.4
10	7.87	8118.90	-22.6	14.72	8910.59	-25.0
30	7.66	8656.39	-19.5	15.59	8253.45	-22.0
100	8.37	6668.58	-16.4	15.30	8653.12	-18.8
300	7.35	9313.94	-12.8	15.81	7379.79	-15.4
1000	8.39	6184.72	-8.9	14.52	8699.07	-11.8
				15.43	6383.33	-7.7

Table 6. Activation energies, Ea, calculated for the low temperature relaxation in GUR1050.

	GUR1050-VE4.4			GUR1050-VE7.9		
Method	**Temperature Range (°C)**	**Activation Energy ($kJ \cdot mol^{-1}$)**	**R^2**	**Temperature Range (°C)**	**Activation Energy ($kJ \cdot mol^{-1}$)**	**R^2**
Havriliak-Negami	-26/-8	192.46	0.9867	-32/-2	202.51	0.9987
Fouss-Kirkwood	-26/-8	182.32	0.9988	-32/-2	184.65	0.9962